Control of magnetism by interfacial strain in Ni/V$_2$O$_3$ nanostructures

Author: Borasino Marqués, Axel.

Advisor: Fraile Rodríguez, Arantxa

Departament de Física de la Matèria Condensada and Institut de Nanociència i Nanotecnologia, Universitat de Barcelona, 08028 Barcelona, Spain

Abstract: Magnetic properties of thin films can be modified through proximity effects with multilayer structures. Materials that undergo both a structural phase transition (SPT) and a metal to insulator transition (MIT) have been used for this purpose. This crystallographic change induces a stress to the adjacent layer that changes the magnetic properties of the film through magnetoelastic anisotropy. This work is devoted to the study of magnetic properties of Ni/V$_2$O$_3$ affected by the SPT of the V$_2$O$_3$. In order to achieve this goal, images obtained with synchrotron-based photoemission electron microscopy have been analyzed to spatially resolve the magnetic domains orientations and observe its evolution with an applied magnetic field. For this purpose-built algorithm has been developed and used in addition to other existing image and data analysis tools. Continuous distributions of coercitivites and magnetizations have been obtained in addition to a rather abrupt magnetic reversal mechanism.

I. INTRODUCTION

One of the still remaining challenges in the field of condensed matter physics is the control and characterization of the magnetic properties of ferromagnetic (FM) layers without the usage of magnetic fields. For this purpose, lately extensive efforts have been devoted to tune the magnetic properties of different layers through external stimulus such as light [1] or electrical fields [2], or by exploiting proximity effects with adjacent materials susceptible to external driving forces such as pressure, stress or temperature [3]. One promising approach exploited for the latter is the study of FM layers, such as Ni, in proximity to materials that undergo a metal-insulator (MT) transition that is concomitant to a structural phase transition (SPT), such as VO$_2$ and V$_2$O$_3$. In this case, both MIT and SPT can be induced by temperature but can also be driven by current, light or pressure [4]. Hence, taking into account the fact that the magnetic properties of the FM layer are altered by its proximity to materials that undergo a MIT and SPT, the control of the magnetic properties of the layer could a priori be reached through multiple external stimuli. These capabilities make of these engineered controlled nanostructures valuable building blocks for technological applications [5].

A recent study has been focused on the changes of magnetic properties of Ni/V$_2$O$_3$ across the SPT of V$_2$O$_3$ [5, 6]. On the SPT, the oxide suffers a crystallographic transition from a high temperature, rhombohedral metallic phase to a low temperature, monoclinic, insulating state. This crystallographic change on the V$_2$O$_3$ results into a reversible modification of the magnetic properties of the FM Ni layer, induced by the magnetoelastic anisotropy caused by the interfacial stress over a narrow temperature window [6] and nanoscale phase coexistence. Large changes in the coercitivity and noticeable modification of the magnetization are the two most prominent changes on the Ni magnetic properties. If the interface roughness between the Ni layer and the V$_2$O$_3$ is of the order of 1-2 nm, a sharper enhancement of the coercitivity coincides with the onset of the first-order V$_2$O$_3$ phase transition.

Although recent simulations based on the magnetic domain wall pinning at V$_2$O$_3$ agree with experimental data, the actual microscopic coupling mechanism is not yet understood. Additionally, using scanning optical microscopy, metal/insulator domains of microns in size have been observed on the V$_2$O$_3$ layers. It has been hypothesized that FM domains may exponentially grow with the predominance of one of the coexisting phases across the SPT from nm to microns. Nevertheless, a direct observation and analysis of the Ni domains and their correlation to the different structural variants (metal/insulator phases) is still missing. This is essential to understand how the strain-mediated coupling mechanism at the interface between the two layers drives the domain wall propagation in the FM film.

In this work, spatially-resolved observation of the FM Ni domains during the underlying SPT has been carried out through the analysis of the images obtained by synchrotron-based photoemission electron microscopy (PEEM) combined with X-ray magnetic circular dichroism (XMCD) [7]. The analysis of the hysteresis curves obtained has required the development of an ad-hoc algorithm in order to normalize and handle the statistically meaningful quantity of data obtained. Thus, the last part of the study has been devoted to the understanding and interpretation of the results. The expected outcomes of the study have been i) characterization of the different Ni domain configurations across the SPT, ii) study of the reversal mechanism domain by domain, iii) analysis of any possible distribution of coercitivites and magnetizations at different temperatures across the SPT.

II. EXPERIMENTAL METHODOLOGY

A. Sample preparation

The sample used for this analysis is made up by a 1012 sapphire substrate above which rests a 100nm-thick V$_2$O$_3$ film with a 10nm Ni layer on its top. The Ni/V$_2$O$_3$ sample has been produced by colleagues at the University of California San Diego (Ivan Schuller's group) using a high-vacuum sputter deposition system with a base pressure of 1x 10^{-7} Torr, similarly to the samples prepared in [1,8]. In order to deposit the 100-nm-thick V$_2$O$_3$ film onto 1012

sapphire substrate, a RF sputtering technique was used with 100 W and a V_2O_3 target in ultra high purity (UHP) Ar gas conditions. In order to achieve the deposit, the temperature was raised to 750 ^{o}C and the pressure was reduced to 4 mTorr. After cooling to room temperature and recovering the base pressure, the Ni film was deposited above the lattice structure. Finally, in order to avoid the oxidation of the structure, a 5 nm Al layer was deposited above the Ni film.
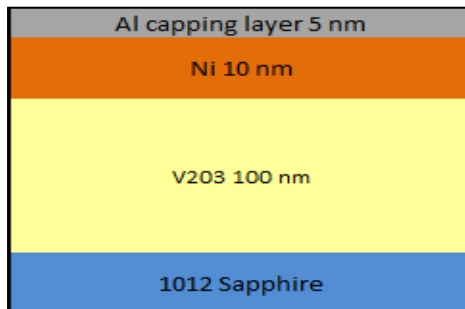

FIG. 1: Cross-section view of the sample.

B. Experiment and data acquisition

The XMCD-PEEM experiment was carried out by the tutor and co-worker at the SPEEM beam line of the HZB-BESSY synchrotron light source in Berlin, Germany. XMCD is based on the difference between two absorption spectra of X-ray with right and left circularly polarized light. The images were obtained through a pixel-wise asymmetry ratio of two PEEM images sequentially recorded with left and right-handed circular polarization at the resonant L3absorption edges of Ni (852.7 eV). In this study the X-ray propagation vector onto the surface was aligned parallel to the [104] crystallographic axis. Finally, the bright and dark grey levels in the images correspond to opposite magnetic orientations. They are the result of the projection of the local magnetization onto the photon propagation vector of the X-rays.

The ferromagnetic Ni domain structure was studied across the structural phase transition (SPT) of the V_2O_3 by recording XMCD images at the resonant L_3 absorption edge of Ni with circular polarization. Thus, the images obtained contain information related to the magnetic properties of the sample, namely the orientation and magnitude of the atomic spins. Taking into account that the SPT of the V_2O_3 occurs near 160K when cooling, the XMCD images were taken along a temperature range of 130 K to 250 K.

The goal of the experiment was to visualize the different orientations of the Ni magnetic domains mediated by stress at the interface with the adjacent V_2O_3 structural variants that are formed while crossing the SPT. In order to do this, element-specific hysteresis loops were done by collecting field dependent XMCD image using a PEEM. Thus the growth mechanism behind the Ni domains and the correlation between the magnetic domains and the underlying crystal systems of the V_2O_3, fully relied on this spatial resolved information.

The study has focused on the analysis of the images corresponding to XMCD-PEEM hysteresis loops with applied magnetic fields up to 500 Oe. Stacks at purely monoclinic phase (146 K), over the phase transition of the V_2O_3 (154 K and 160 K) and at high temperature corresponding to purely rhombohedral phase (200 K) were carried out. In order to gain statistically significant results, an average number of 4 hysteresis loops per temperature were performed.

Earlier studies have pointed out and demonstrate the coercitivity enhancement of Ni/ V_2O_3 bilayers caused by the SPT of the vanadium oxide. It has been pointed out that the magnetic coercitivity of the sample is inversely proportional to temperature. This result anticipates that a lower value of the applied magnetic field is needed for saturating the sample. Hence, the range of the applied field at low temperature stacks (146 K) is larger than the one needed for the 200 K stacks. Technical parameters about the experiment can be seen on Table I.

Temperature ± 0.5 (K)	H_{min} (Oe)	H_{max}(Oe)
200.0	133.3	266
160.0	200	366
	200	433
154.0	266	433
146.0	333	500
	266	500

TABLE I: Applied magnetic fields for each temperature along the SPT. On the 146 and 160, three stacks were obtained using the upper range and only one with the lower case. All the cycles had an interval of 6.67 Oe between two Images.

C. Image analysis

The first part of the analysis was devoted to recognize and identify the magnetic inversed domains. The gray scale XMCD images obtained by the above experimental procedure had a field of view of 10 μm x 10 μm (corresponding to 512x512 pixels) that allowed us distinguish the different magnetic orientation of a fair number of individual Ni domains. For statistics, 4-5 hysteresis loops were recorded for each temperature (146 K, 154 K, 160 K and 200 K). In order to ensure a reference point to equally analyze all the stacks, the images were aligned with the PEEMvision software tool [9]. A black spot on the middle of the image served us to correctly align the images. Due to drifts between subsequent images in the stack, the centre of the image sequence tended to move to the bottom right corner and thus, the available region for identifying and characterize Ni domains decreased. Hence, the first limitation factor of this analysis was the loss on the final image available dimensions after the alignment. Right after, the histogram of the images was equalized in order to improve the contrast, and consequently the detection of inverted domains. Fig.(2) shows how the contrast was enhanced through an equalization of the histogram. The tool used for the image processing was ImageJ [10]. The inverted domains have been detected on the images as regions with a darker level of intensity in its pixels. Techniques such as the binarization were rejected from the

*Electronic address: boma.axel@gmail.com

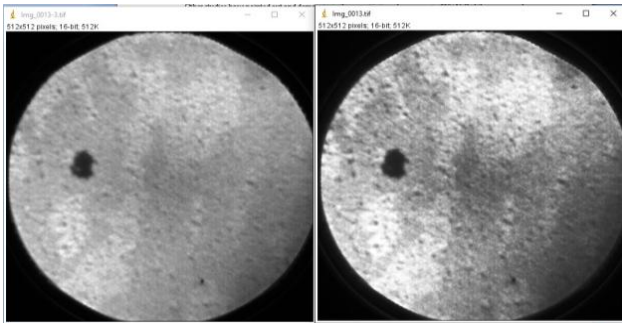analysis due to its inability to detect the possible sequentially mechanism of domain inversions.

FIG. 2: Standard and histogram equalized images, left and right respectively, corresponding to 160K with a H = 180 Oe.

Rather than analysing the images pixel per pixel, an analysis of a region of interest (ROI) was made with the aim of increasing the signal to noise ratio (SNR). For each stack, an average number of 20 regions of interest (ROIs) were selected. Each ROI corresponded to an individual magnetic domain. The intensity value of each ROI was calculated as the mean value of the pixels therein. The selected ROI's tried to be large enough to group a significant number of pixels but sufficiently small to avoid reaching non-inverted regions. The most prominent factor limiting the image analysis was the inhomogeneous illumination of the images, both between different images in the stack as well as across the field of view in the single images. Such a lack of homogeneous illumination was a consequence of measuring under magnetic fields. These fields modified the trajectory of the photoelectrons in the PEEM microscope, causing an inhomogeneous spatial distribution of the collected photoelectrons within the measured field of view. Whereas different measurement and software-based tools were used to correct this phenomenon, none of them was good enough to fully avoid it.

Once the ROIs were selected, the Python algorithm was applied in order to normalize the magnetizations from 0 to 1 (from non-inverted to inverted domain). With this algorithm some of the previously selected ROIs were rejected due to the impossibility of discerning between the lighting drift and the magnetic reversal mechanism itself. The criterium used for this was based on a fixed threshold that the grayscale amplitude of the inverted domains inside each ROI had to overcome to ensure that they were not artefacts of a poor illumination. An additional manual analysis was also performed in critical ROIs with very low SNR. The ad-hoc algorithm was implemented in Python [11] and scaled all the ROIs of a certain temperature according to the value of its jump (mean value of its ROI grayscale intensity before and after the inversion). Then the algorithm rescaled all the curves belonging to that temperature according to the maximum magnetization value. Once the grayscale amplitude of the Ni inverted domains was determined, an interpolation was done to the points before and after the inversion in order to reduce the drift caused by the illumination. This interpolation was justified due to the fact that the magnetic domains could not reverse its orientation several times.

III. RESULTS AND DISCUSSION

In general traits, it is observed that the SPT in V_2O_3 induces nucleation of Ni domains, and their fraction grows monotonically with the predominance of one of the coexisting structural phases. Furthermore, the domain nucleation sites are randomly distributed across the sample for several image series, indicating that the domains are not pinned by structural defects. As can be seen on Fig.(3), a continuous range of coercitivites has been extracted for each temperature.
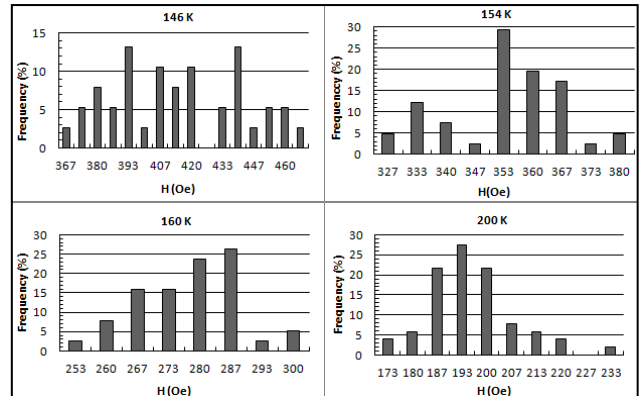

FIG. 3: Histograms corresponding to 146K (upper-left side), 154K (upper-right side), 160K (bottom-left side) and 200K (bottom-right side). These histograms were obtained with the number of ROIs that start to invert along the magnetic field applied.

As the temperature decreases, the centre of the distribution is shifted towards higher coercivity values, in agreement with earlier MOKE measurements [6,8]. Furthermore, Ni inverted domains formed above the monoclinic crystallographic phase have a wider distribution of coercitivities in contrast with the purely rhombohedral phase at high temperature. An intermediate behaviour between these two regimes takes place at temperatures of 154 K and 160 K, i.e. around the SPT. The reason for this is the evolution with temperature of the number and characteristics of the structural variants from the two crystallographic phases of the proximal V_2O_3 layer that are produced during the SPT. Furthermore, as expected, the number of nucleated domains increases with the magnetic field, and after reaching a maximum value, the population drops. This can be explained through a combination of Ni domain growth modes, nucleation, coalescence and propagation, due to the fact that the initially nucleated Ni domains merged to a finally big cluster where the entire domains were already inverted. For some of the temperatures studied, in particular the 200 K, the population of inverted domains is quite correlated with a Gaussian profile.

Another crucial point of this study was to analyse the inversion mechanism of the domains. Fig.(4) shows the hysteresis loops of a number of Ni single domains at four different temperatures. In general traits, all the Ni domains

*Electronic address: boma.axel@gmail.com

studied changed their magnetic orientation between steps of 7 and 13 Oe and suffer an abrupt drop on its magnetic orientations. It should be noted that if instead of 7 Oe between consecutive images, a smaller step was used, it could be that the analysis would have been sensitive to a more progressive inversion mechanism. Note that some of the ROIs at 160 K seem to suggest a sequential inversion mechanism (i.e inversion of the magnetic orientation of the domain with steps larger than 13.3Oe). However, since these observations were hindered by the very low SNR of the corresponding ROIs, these magnetic domains have finally been excluded from the study.
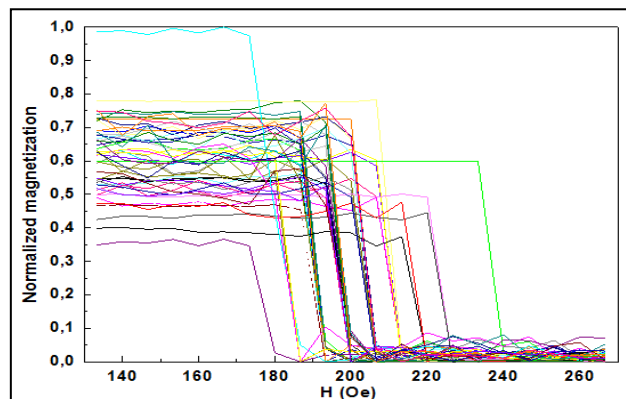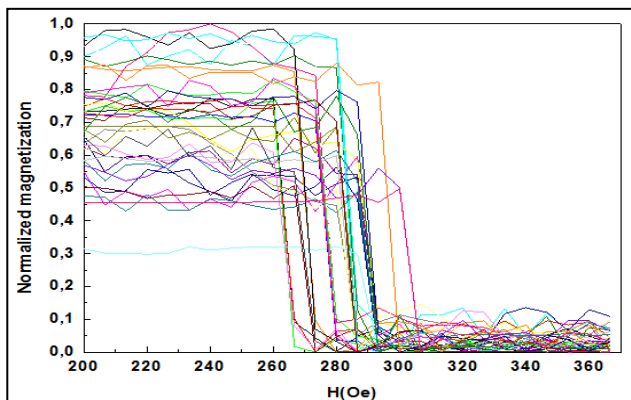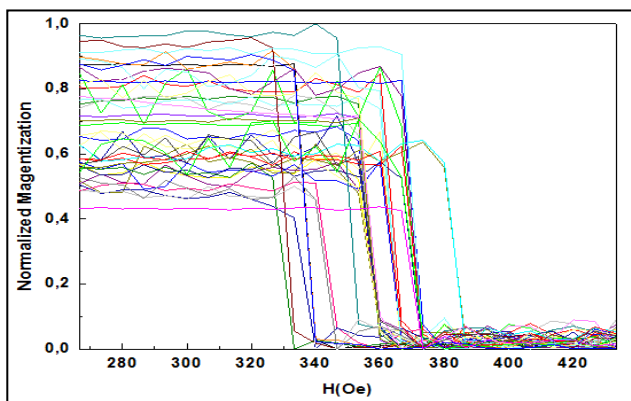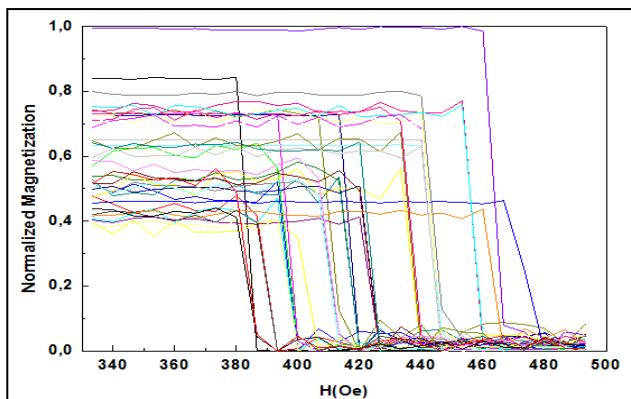

FIG. 4: From top to bottom, hysteresis loops corresponding to 146 K, 154 K, 160 K and 200 K. Each of the curves represents a ROI that is normalized according to its percentage with the highest jump at that temperature. The jump is the difference value of the pixels before and after the inversion of the domain. A wider distribution of the coercitivites corresponding to 146K can be noted here as well.

Finally, the last objective of the study was to understand the possible distribution of magnetization values. According to the general decrease of the permanent magnetization of the samples along the temperatures, different distributions were obtained on Fig.(5). Despite some differences between the temperatures, an overlay Gaussian behaviour can be extracted taking into account the limitation factors expressed before. Therefore, the distribution of magnetization values can be described through a normal statistical distribution. However, information about the relationship of the μ factors of each normal distribution with the temperature needs an individual study per se. Nevertheless, it can be seen that the centre of the Gaussian distribution (μ factor) changes along the temperatures.
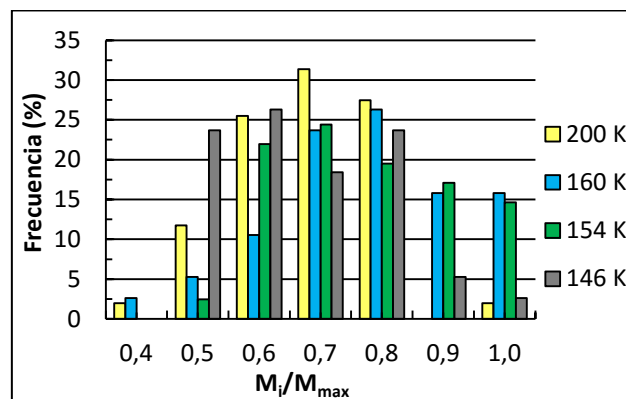

FIG. 5: Histogram corresponding to the magnetization distribution along the temperatures. The x-axis represents the proportion of magnetizations with respect to the maximum magnetization for that temperature. It can be noted that the most probable magnetization values fall into the 70% of the total magnetization value for a given temperature.

*Electronic address: boma.axel@gmail.com

IV.   CONCLUSIONS

As a summary, the results of the present study have shown the change and distribution of the magnetic properties of the Ni film due to the SPT and MIT on the V_2O_3. The idea was to analyze the magnetic properties of the Ni domains with a predominant crystallographic phase, either monoclinic (146 K) or rhombohedral (200 K), in order to better understand the magnetic features of the sample with the coexistence of both phases (150 K &160 K). In addition, the Python algorithm developed for this study has been very valuable to handle the large quantity of the data obtained from the image analysis and has provided valuable outcomes.

On one hand, a distribution of coercitivities has been obtained through a ROIs study of different temperatures of the sample. Domains formed above the monoclinic crystallographic phase have a wider distribution of coercitivites in contrast with the purely rhombohedral phase at high temperature. An intermediate behaviour between these two regimes takes place between the temperatures of 154 K and 160K due to the coexistence of the two structural phases. On the other hand, the shape of the hysteresis loops of the individual domains indicates an abrupt change of the magnetization in a relatively low field range. This is indicative of a fast propagation of domain walls. The limitations of the experimental device have not allowed a more deeply study of this phenomenon, but due to the statistically meaningful quantity of data extracted, this kind of inversion seems to rule the transition.

To conclude, a roughly Gaussian distribution of magnetizations has been retrieved. The existence of magnetization and coercitivity distributions confirms previous MOKE measures where an enhancement of the coercitivity was discovered. It can be seen how this normal statistical distribution depends on the temperatures studied but a deeper and more sophisticated analysis should be performed in order to extract more consistent results.

V.   OUTLOOK

The analysis of the lateral correlation length of the inverted domains is currently under study. This should help establishing whether the predominant growth phenomenon is nucleation of isolated domains or coalescence of existing closely-located regions.

Acknowledgments

_____

[1] A. Kirilyukm, A.V. Kimel and T. Rasing, *Rev. Mod. Phys*., p 82, 2731, 2010.

[2] L.P. Rokhinson, M.Overby, A. Chernyshov, Y.Lyanda-Geller, X.Liu, and J.K. Furdyna, *J. Magn. Magn.Mater*., p 324, 3379, 2012.

[3] S. Saranu, S. Selve, L. Han, U. Wiedwald, P. Ziemann and U. Herr, Beilstein *J. Nanotechnology*., pp 268-275, 2, 2011.

[4] M. Imada, A. Fujimori, and Y.Tokura, *Rev. Mod. Phys*., p 70, 1039, 1998.

[5] Y. Hwang, Y. Iwasa, M. Kawasaki, B. Keimer, N.Nagaosa, and Y.Tokura, *Nat. Mater*., p 11, 103, 2012.

[6] J. de-la-Venta, S. Wang, J. G. Ramirez, and I. K. Schuller, *Appl. Phys. Lett*., 102, 122404, 2013.

[7] J.Stöhr and H. Siegmann, Magnetism: From fundamentals to Nanoscale Dynamics, *Springer Series Solid Science*, 2007.

[8] J. de-la-Venta, S. Wang, T. Saerbeck, J. G Ramírez, I. Valmianski, and I. K. Schuller, *Appl. Phys. Lett*., 104, 062410, 2014.

[9] A. Scholl. Available at: http://xraysweb.lbl.gov/peem2/webpage/Tools.shtml

[10] Rasband, W.S., ImageJ, U. S. National Institutes of Health, Bethesda, Maryland, USA. Available at: http://imagej.nih.gov/ij/, 1997-2016.

[11] Python Software Foundation. Python Language Reference, version 2.7. Available at: http://www.python.org

*Electronic address: boma.axel@gmail.com